

1 of 1

10/22/93 JSD

Conf. 921122-67

SLAC-PUB-5970
October 1992
(E)

**PERFORMANCE OF A SILICON CCD PIXEL VERTEX DETECTOR
IN THE SLD ***

THE SLD COLLABORATION

*Stanford Linear Accelerator Center
Stanford University, Stanford, California 94309*

Represented by

M. G. Strauss
*University of Massachusetts
Amherst, Massachusetts 01003 USA*

ABSTRACT

We present first results on the performance of a CCD based silicon vertex detector operated in 1992 in the SLC Large Detector (SLD) at the SLAC Linear Collider (SLC). A sample of 11K polarized Z^0 decays have been analyzed. Results on operational experience, alignment techniques, beam and detector backgrounds, and mechanical and thermal stability are presented. In conjunction with the central drift chamber, we present data on tracking and vertexing efficiency, and impact resolution for Z^0 events.

*Presented at Particles & Fields 92:
7th Meeting of the Division of Particles and Fields of the APS (DPF 92),
Batavia, IL, November 10-14, 1992*

*Work supported in part by the U.S. Department of Energy under contract DE-AC03-76SF00515 (SLAC).

MASTER

Se

DISTRIBUTION OF THIS DOCUMENT IS UNLIMITED

1. Introduction

The SLC is an excellent environment to study the decay of heavy particles with lifetimes on the order of $10^{-13} - 10^{-12}$ seconds, due to the small transverse size of the interaction point ($\approx 2 \mu\text{m}$), and the beam pipe radius (25 mm). To fully exploit these studies, we have built a CCD-based Vertex Detector (VXD), which gives excellent 3-dimensional track resolutions. Unlike silicon strip detectors, this device gives comparable resolutions along both axes in the plane of the detector. Also, in contrast to cross strips, there are no combinatoric ambiguities, so higher track densities and backgrounds can be tolerated and pattern recognition is more effective.

As described in previous publications,^{1,2} the VXD consists of 480 charge coupled devices (CCDs) installed around the beam pipe. A CCD contains $\approx 400 \times 600$ pixels, each of size $22 \times 22 \mu\text{m}$, and has an active area of $8.5 \times 12.7 \text{ mm}^2$. Eight CCDs are wire-bonded to an alumina mother board of thickness 250 μm to create a CCD "ladder" with an active area of about $8.5 \times 100 \text{ mm}^2$. These ladders are arranged in four coaxial cylindrical layers, located at nominal radii of 29.5, 33.5, 37.5, and 41.5 mm around the beam pipe. The inner (outer) two layers contain 13 (17) ladders each. The ladders are mounted in two half cylindrical beryllium support structures with spring-loaded fixtures. During construction, the relative locations of all CCDs on a single ladder were optically surveyed with an accuracy of 5 μm at the operating temperature of -80°C . The location of CCDs on different ladders was optically surveyed to $\approx 10 \mu$. Each ladder extends to approximately $\pm 4.6 \text{ cm}$ along the direction of the beam axis. The inner (outer) layer subtends a range of $|\cos \theta| < .85 (< .75)$. The VXD covers about 75% of 4π . A drawing of the vertex detector is shown in Figure 1.

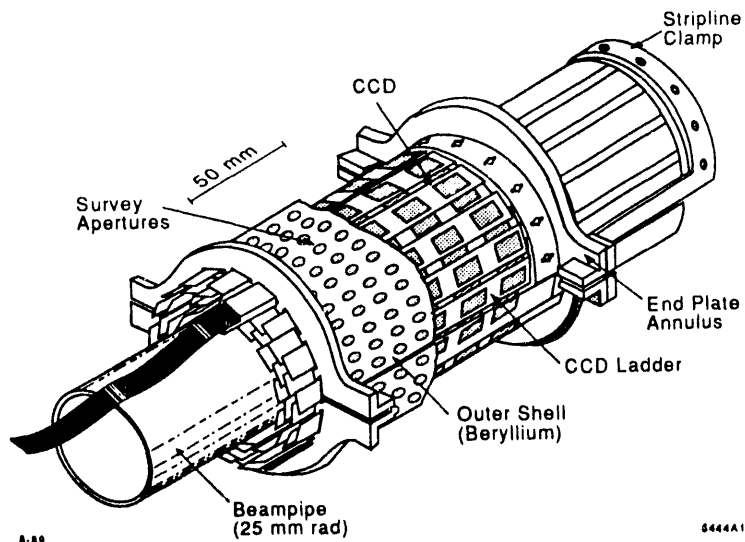


FIGURE 1: Artist's drawing of the SLD Vertex Detector

The CCDs are surrounded by a foam cryostat and are cooled by flowing N_2

gas through the detector. Cooling the detector suppresses dark currents and the loss of CCD charge transfer efficiency from radiation damage. Electronic readout is accomplished by clocking the CCD charge to an output node at 1.85 MHz. All CCDs are read out in parallel, continuously. Total readout time is 160 ms corresponding to 19 beam crossings. This slow readout does not impose any dead time, but does increase the background in the VXD by the corresponding factor. The increased background does not, however, present a serious problem due to the very high granularity of the detector.

2. Pattern Recognition

Charged particles traversing the VXD and central drift chamber (CDC) are first identified as tracks in the CDC. Two methods are used to associate the CDC tracks with hits in the VXD. For both methods, the CDC track parameters are extrapolated back to the VXD and an elliptical search area for VXD hits, dependent on momentum, is established. In the first method, the tracks are constrained to go through the nominal interaction point, while in the second method no constraint is imposed. Typically, this "primary" search area ranges from about 5-25 mm along the direction of the beam axis (Z direction), and from 0.5-4 mm perpendicular to both the beam and the radial direction (R- ϕ direction). Candidate hits in the search area are included in a new track fit, and a "secondary" search is made to find other hits at smaller radii which link with the CDC track and the first candidate hit. This secondary hit search area is usually limited to a few hundred μm in both the Z and R- ϕ directions. A fit is then performed for all track candidates with two or more VXD hits at different radii. Tracks with good χ^2 are retained.

3. Operational Experience

The SLD vertex detector was installed and commissioned in April 1992. Altogether, 94% of the 480 channels have proven to be functional and reliable; 4% have electronics problems and give no charge read out; 2% have intermittent electronic problems.

Backgrounds in the detector come predominately from X-ray conversions and up-stream tracks parallel to the beam pipe axis. The X-ray hits deposit many times minimum ionizing energies. The parallel track backgrounds are suppressed by deleting clusters having a large number of hit pixels. Electronic noise is minimal, less than 1 hit/CCD for each event. All backgrounds add up to less than .01% occupancy in the detector. Monte Carlo studies indicate that the effect of these backgrounds is to cause about 4% of the CDC tracks with $p < 1 \text{ GeV}/c$ to have incorrect clusters associated with them in the VXD. For tracks with $p > 1 \text{ GeV}/c$, this number decreases to < 0.5%.

To achieve a global spatial resolution of $10 \mu\text{m}$, the results from the optical survey were refined by using CDC tracks linked to ≥ 3 VXD hits. Minimizing the residuals and correlations on these three point tracks allows small corrections to be

made to the survey whose accuracy is reflected in the track spatial resolutions (see section 5). The temporal and thermal stability of the VXD location with respect to the CDC is checked by monitoring capacitive probes and precision potentiometers attached to the detector. These measurements show that the VXD location is constant to $\pm 5 \mu\text{m}$ in the transverse direction.

4. Cluster Finding and Track Linking Efficiencies

The efficiency for collecting charge on the CCDs and forming a VXD cluster, or hit, is determined using CDC tracks with $p > 1 \text{ GeV}/c$. These tracks are constrained to go through the primary interaction point. The constrained tracks are extrapolated to each of the four layers and a search for nearby clusters is made where the track intersects an active CCD. The CCDs along the extrapolated track are considered to be inefficient if no two clusters coincidentally fit to the track. Background subtraction is done by repeating this procedure with tracks from one Z^0 event and CCD hits from a different Z^0 event. The efficiency for finding clusters from charged tracks is measured to be $99 \pm 1\%$.

The efficiency for linking VXD points with CDC tracks is measured using CDC tracks with $p > 1 \text{ GeV}/c$ which extrapolate to within 1 cm in Z and 2 mm in XY from the primary interaction point, where XY is the plane perpendicular to the beam axis. In regions where all the CCDs are active, 96% are linked (Figure 2).

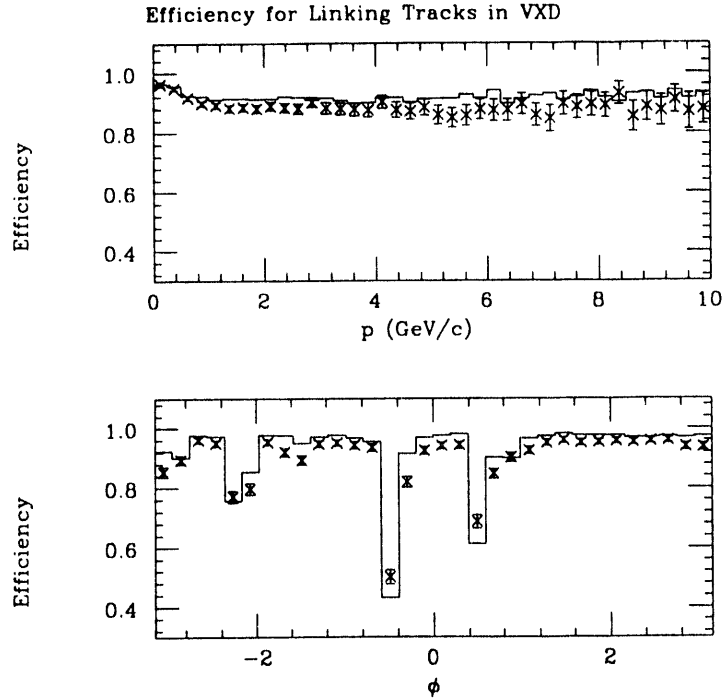


FIGURE 2: Efficiency for linking CDC tracks with VXD hits. The points are from data and the histogram is from Monte Carlo.

5. Spatial Resolutions and Impact Parameters

The tracking spatial resolution is measured using CDC tracks with three hits in the VXD. A fit is made to the track using only the VXD hits at the minimum and maximum radii. The residual between the third hit and the fitted track have widths $\sqrt{2}$ times the single CCD tracking precision, plus additional effects due to survey errors. When two of the three hits are on the same ladder, a single CCD spatial resolution of $5 \mu\text{m}$ in the XY plane and $8 \mu\text{m}$ in the RZ plane is measured (Figure 3). When all three hits are on different ladders, the global spatial resolution is measured to be $10 \mu\text{m}$ in XY and $8 \mu\text{m}$ in RZ. There are still long range geometric distortions which, when corrected for, should decrease these numbers.

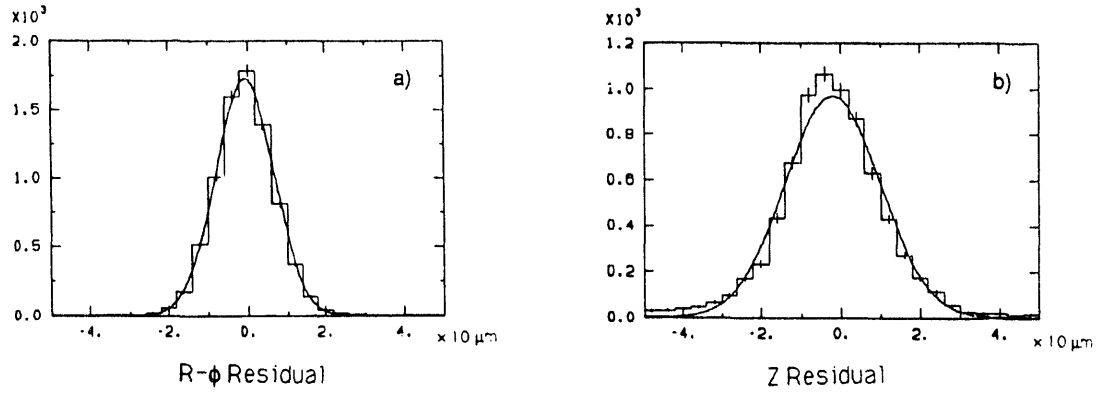


FIGURE 3: Tracking precision as determined by single ladder residuals in the a) R- ϕ plane and b) R-Z plane. Lines are Gaussian fits.

The two track impact parameter has been measured for high momentum tracks using muon pairs from Z^0 decays. The tracks are extrapolated to the point of closest approach to the nominal interaction point and the distance between them is computed. Gaussian fits give single track resolutions of $13 \mu\text{m}$ in XY, and $52 \mu\text{m}$ in RZ (Figure 4). When a term for multiple scattering is included, the error on the impact parameter for tracks perpendicular to the beam line can be approximated by

$$\sigma_b(\text{XY}) = \sqrt{13^2 + (70/p)^2} \quad \text{and} \quad \sigma_b(\text{RZ}) = \sqrt{52^2 + (70/p)^2} ,$$

where σ_b is in microns, p is the track momentum in GeV/c .

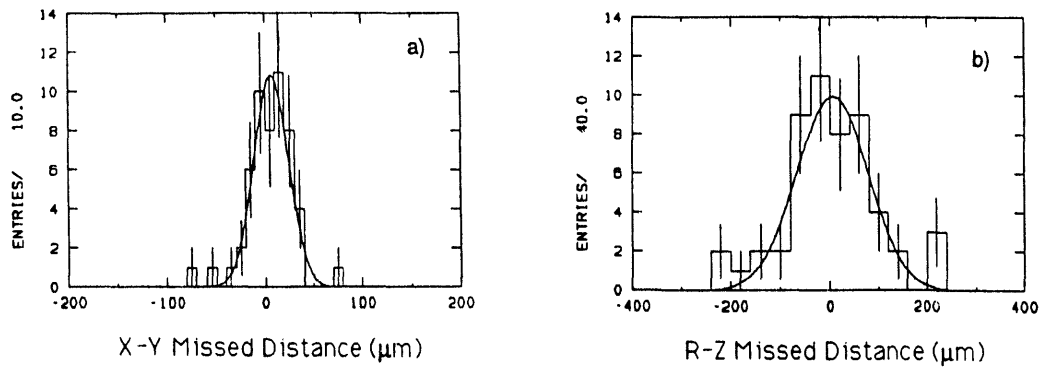


FIGURE 4: σ_b for high momentum tracks as determined by the muon pair missed distance in the a) $R-\phi$ plane, and the b) $R-Z$ plane. Lines are Gaussian fits.

1. C.J.S. Damerell et.al., *Nucl. Inst. Meth. Phys. Res. A* **288** (1990) 236-239.
2. G.D. Agnew et.al., *Proc. XXVI Intern. Conf. on HEP, Dallas, Texas* (1992).

DISCLAIMER

This report was prepared as an account of work sponsored by an agency of the United States Government. Neither the United States Government nor any agency thereof, nor any of their employees, makes any warranty, express or implied, or assumes any legal liability or responsibility for the accuracy, completeness, or usefulness of any information, apparatus, product, or process disclosed, or represents that its use would not infringe privately owned rights. Reference herein to any specific commercial product, process, or service by trade name, trademark, manufacturer, or otherwise does not necessarily constitute or imply its endorsement, recommendation, or favoring by the United States Government or any agency thereof. The views and opinions of authors expressed herein do not necessarily state or reflect those of the United States Government or any agency thereof.

**DATE
FILMED**

2/3/94

END

